

Relativistic Winds from Compact Gamma-Ray Sources: II. Pair Loading and Radiative Acceleration in Gamma-ray Bursts

Christopher Thompson¹ and Piero Madau^{2,3}

ABSTRACT

We consider the effects of rapid pair creation by an intense pulse of γ -rays propagating ahead of a relativistic shock. Side-scattered photons colliding with the main γ -ray beam amplify the density of scattering charges. The acceleration rate of the pair-loaded medium is calculated, and its limiting bulk Lorentz factor related to the spectrum and compactness of the photon source. One obtains, as a result, a definite prediction for the relative inertia in baryons and pairs. The deceleration of a relativistic shock in the moving medium, and the resulting synchrotron emissivity, are compared with existing results for a static medium. The radiative efficiency is increased dramatically by pair loading. When the initial ambient density exceeds a critical value, the scattering depth traversed by the main γ -ray pulse rises above unity, and the pulse is broadened. This sets an upper limit to the pre-burst mass loss rate of $\sim 10^{-5} M_{\odot}$ per year, and places significant constraints on gamma-ray burst progenitors. An anisotropic γ -ray flux (on an angular scale Γ^{-1} or larger) drives a large velocity shear that greatly increases the energy in the seed magnetic field forward of the propagating shock.

Subject headings: gamma-rays: bursts – theory – radiation mechanisms

1. Introduction

Physical models for γ -ray emission from a relativistic fireball, and the ensuing synchrotron emission from the decelerating shock, have generally neglected the feedback of the intense γ -ray flux on the dynamics of the fireball, or on the prompt and delayed emission. There are, however, several reasons to believe that this interaction can have an important influence on the observed multiwavelength emission from gamma-ray bursts (GRBs). Pair creation by high energy photons will raise the radiative efficiency of a shock (Thompson 1997); and – if the ambient medium is sufficiently dense – it will significantly smear and broaden the observed time profile of the prompt GRB. The pairs also carry net forward momentum which will couple effectively to the ambient

¹Department of Physics and Astronomy, University of North Carolina, Chapel Hill, NC 27599.

²Institute of Astronomy, Madingley Road, Cambridge CB3 0HA, UK.

³Institute for Theoretical Physics, University of California, Santa Barbara, CA 93106–4030.

medium if this contains a strong enough magnetic field. In this work we extend previous results on radiative acceleration in the Thomson (Noerdlinger 1974; O’Dell 1981; Phinney 1982; Kovner 1984) and Klein-Nishina (Madau & Thompson 1999, hereafter Paper I) scattering regimes to include the effects of pair creation. Attenuation of the high energy γ -ray spectrum by collisions with soft photons was calculated by Baring and Harding (1997), but the dynamical effects of pair creation and the feedback of radiative acceleration on the scattering depth were not considered in that work. The role of pair creation in accelerating a trans-relativistic outflow from a black-hole accretion disk with a hard X-ray spectrum has been considered recently by Beloborodov (1999).

The plan of this paper is as follows. In §2 we calculate the rate of acceleration by a thin shell of γ -rays, some of which side-scatter off ambient charges and collide with the main γ -ray beam. We show that acceleration is much faster (for a given compactness) than in the Thomson limit, because the highest energy photons provide most of the momentum. The reduction in the mean inertia per scattering accompanying pair creation significantly increases the limiting Lorentz factor over the value for a baryonic plasma. In §3 we apply these results to GRB afterglows. We consider the deceleration of a relativistic shock propagating into a medium that is itself moving at bulk relativistic speed, and show how the time scaling of the synchrotron emission is modified from the case of a static medium. We estimate the limiting ambient density above which the γ -ray pulse experiences a large optical depth to scattering. Finally, we note that angular variations in the radiative force will excite non-radial shear flows in the ambient medium that can greatly amplify the pre-existing seed magnetic field.

In the following we will denote by x and x_s the incident and scattered photon energies in units of $m_e c^2$ in the (unprimed) lab frame, and with $\Gamma = (1 - \beta^2)^{-1/2}$ the bulk Lorentz factor of the flow.

2. Pair loading

Gamma-ray sources of high compactness are opaque to photons that move at an angle with respect to the γ -ray flow. When the source spectrum extends to an energy $x \gg 1$, even soft photons will create pairs via $\gamma\gamma \rightarrow e^+e^-$, with a cross-section close to Thomson near threshold. This implies that the source of γ -ray radiation must itself expand at relativistic speed. When the photons are beamed into a narrow angle θ along the direction of motion, the threshold energy for pair production within the beam is increased to $x \sim \theta^{-1}$. In Paper I we calculated the radiative acceleration of matter exposed to a strong source of γ -rays, including the full Klein-Nishina suppression of the scattering cross-section, but did not include the effects of pair creation. However, the same Compton scattering process that accelerates material sitting close to a γ -ray source also creates side-moving photons. When the integrated flux of photons of energy $x \geq 1$ is large, each side-scattered photon deposits its *entire* momentum, along with the momentum of a second colliding photon, into an electron-positron pair. The build-up of a pair plasma (‘pair loading’) through this process, and the bulk acceleration that ensues, will be the subject of this section.

2.1. Radiative Acceleration

At very high compactness, the source of gamma-rays must be impulsive; otherwise the assumption of low scattering optical depth in the accelerating medium is not self-consistent. We approximate the photon source as a radially propagating shell situated at $c(t - \Delta t) < r < ct$. We found in Paper I that, in the Thomson limit, a test particle surfing the photon shell attains a limiting Lorentz factor

$$\Gamma_{\max} = \frac{\tau_c}{2} \left(\frac{m_e}{\mu} \right) \quad (1)$$

when the shell is thin enough that the acceleration length is much less than the radius,

$$\frac{2}{3}\Gamma_{\max}^2 c\Delta t \ll r. \quad (2)$$

The parameter

$$\tau_c \equiv \sigma_T \Delta t \frac{F}{m_e c^2}, \quad (3)$$

is expressed in terms of the integrated energy flux

$$F = \int F_x dx, \quad (4)$$

and characterizes the column density of photons N_γ through the shell, $\tau_c \sim \sigma_T N_\gamma \langle x \rangle$. When the particles are coupled by a magnetic field and the electrons and positrons are cold, the mean mass per scattering charge is

$$\mu = m_e + m_p \left(1 + 2 \frac{n_{e^+}}{n_p} \right)^{-1}. \quad (5)$$

(We assume for simplicity a hydrogen plasma and neglect the inertia of the original neutralizing electron component, but not of the pairs.) The term m_e in this expression must be replaced with the relativistic inertia $\mu_e \equiv \frac{4}{3} \langle \gamma_e \rangle m_e$ when the electrons and positrons are hot.

The optical depth to pair creation is proportional to the optical depth parameter τ_c , which is in turn proportional to the duration Δt of the gamma-ray pulse, and the source compactness $L\sigma_T/(4\pi\mu c^3 R)$. Here, R and L are the source radius and luminosity, respectively. We assume that the incident spectrum is broadband, extending well above and below $x \sim 1$. As long as $\tau_c \gg 1$, even a soft photon that is side-scattered can be absorbed by the main photon beam. The accelerating material is, in this situation, *photon rich*: a side-scattered photon that finds itself above the pair creation threshold has a much higher probability of colliding with another photon than of Compton scattering a second time. Indeed, the number of scattering particles in the relativistically expanding material that emits the photons is suppressed by a factor of Γ^{-1} with respect to the number of photons.

We now calculate the momentum deposited when a (soft) photon B is side-scattered through an angle θ_s and collides with a (hard) photon A . The combined process of scattering followed by pair creation deposits a net forward momentum $(x^A + x^B)m_e c$ in the accelerating medium.

When the scattering charge is cold, the initial energy of the scattered photon in the rest frame of the scattering charge is $x' = x\Gamma(1 - \beta)$. A similar relation, $x'_s = x_s\Gamma(1 - \beta \cos \theta'_s)$, holds for the photon after scattering. The scattering angle in the frame of the charge is given by $\cos \theta'_s = (\cos \theta_s - \beta)/(1 - \beta \cos \theta_s)$. The lab frame energy x^B before scattering can be related to the energy x_s^B following scattering through

$$x^B = \frac{\Gamma x_s^B (1 - \beta \cos \theta_s)}{(1 - \beta)\Gamma - (1 - \cos \theta_s)x_s^B}, \quad (6)$$

which approaches $x^B \rightarrow x_s^B(1 - \beta \cos \theta_s)/(1 - \beta)$ in the Thomson limit ($x' = x'_s$). In these variables, the cross-section for the collision between photons A and B (scattered) is

$$\sigma_{\gamma\gamma} = \frac{3}{16}\sigma_T(1 - \xi^2) \left[(3 - \xi^4) \ln \left(\frac{1 + \xi}{1 - \xi} \right) - 2\xi(2 - \xi^2) \right] \quad (7)$$

(Jauch & Rohrlich 1976), where

$$\xi = \sqrt{1 - \frac{2}{x^A x_s^B (1 - \cos \theta_s)}}. \quad (8)$$

The cross-section reaches a maximum of $0.25\sigma_T$ at $x^A = 2x_{\min}^A$ ($\xi = 0.71$).

Most of the momentum deposited through this process involves the side-scattering of very soft photons, which collide with hard gamma-rays to produce energetic (and almost radially moving) pairs. The minimum (threshold) energy of the radial photon can be expressed as a function of the energy and propagation angle of the side-scattered photon,

$$x_{\min}^A(x_s^B, \theta_s) = \frac{2}{x_s^B(1 - \cos \theta_s)}. \quad (9)$$

Thus, a photon of energy $x_s^B \ll \langle x \rangle$ that is side-scattered through an angle $\sim \theta_s$ creates a pair of energy $x^{\text{pair}} \sim 4/\theta_s^2 x_s^B$. During the first stages of the acceleration, this pair will be relativistic in the bulk frame,

$$2\gamma_e(\text{injected}) \sim \frac{x^{\text{pair}}}{(1 + \beta)\Gamma} \gg 1. \quad (10)$$

(Recall that the photon beam is assumed to be radially streaming.)

In the presence of a sufficiently strong magnetic field, this momentum is effectively communicated to the other charges. Inspection of eq. (37) in Paper I shows that this coupling rapidly becomes stronger as Γ increases. In the case of a γ -ray fireball of duration $\Delta t \sim 10$ s and photon optical depth $\tau_c \sim 300$ (eq. [3]), propagating into an interstellar medium with $B_0 \sim 3 \times 10^{-6}$ G, the coupling is strong only for pairs of lab frame energy $x^{\text{pair}} \sim \text{few}$. However, above a Lorentz factor

$$\Gamma \sim 3.5 \left(\frac{B_0}{3 \times 10^{-6} \text{ G}} \right)^{-1/5} \left(\frac{\tau_c/\Delta t}{30 \text{ s}^{-1}} \right)^{1/5} \left(\frac{x^{\text{pair}}}{100} \right)^{2/5} \quad (11)$$

even energetic pairs deposit their entire momentum. In the process, all particles will share a bulk radial Lorentz factor. In the calculations that follow, we assume that B_0 is strong enough (and Δt long enough) to assure effective coupling; but this constraint should be kept in mind when applying the formulae below.

When $\tau_c \gg 1$, each newly created e^+e^- Compton cools on the main photon beam. Indeed, it drops to an energy far below the injection energy over the time that the medium accelerates; this starting assumption will be justified *a posteriori* in §2.2. In the process of scattering off an anisotropic radiation field, the cooling particle absorbs an additional momentum – similarly to what happens in the Compton rocket (O’Dell 1981; Phinney 1982). The effect of this *Compton afterburn* on the net momentum deposited in the medium depends on whether the Compton-scattered photons are absorbed by pair creation. When they are not absorbed, the net effect is to increase the total momentum absorbed per photon collision to

$$f \times (x^A + x^B)m_e c. \quad (12)$$

Because the magnetic field becomes nearly transverse as the medium accelerates, the numerical factor works out to $f = \frac{5}{3}$ (Paper I). Secondary pair creation can be neglected after the bulk Lorentz factor reaches a critical value, but during the early stages of the acceleration the side-scattered photons are absorbed. The net effect then is to cancel the additional momentum absorbed by the cooling charge, and to force $f \rightarrow 1$. We discuss further details of the pair-photon cascade induced by the injection of an energetic pair in §2.3, and for now summarize this process in terms of mean relativistic inertia $\mu_e \simeq \frac{4}{3}\langle\gamma_e\rangle m_e$ of the daughter e^\pm , and a multiplicity factor N_{mult} . When secondary pair creation can be neglected, one has $N_{\text{mult}} \simeq 1$; otherwise

$$2\langle\gamma_e\rangle N_{\text{mult}} \simeq \frac{x^A + x^B}{(1 + \beta)\Gamma}. \quad (13)$$

The quantity on the RHS is the total energy of the injected pair in the bulk frame.

Let us now calculate the rate of acceleration due to injection of energetic pairs which cool down rapidly off the main photon beam, to a mean Lorentz factor $\langle\gamma_e\rangle \ll \langle x^A + x^B \rangle$. In the fluid approximation the rate of change of the bulk momentum is given by

$$\begin{aligned} \frac{\partial}{\partial t} \left[\Gamma^2 \beta c (2\mu_e n'_{e^+} + m_p n'_p) \right] + \nabla \cdot \left[\beta \Gamma^2 \beta c^2 (2\mu_e n'_{e^+} + m_p n'_p) \right] = \\ \int (x^A + x^B) f \frac{F_x(x^A)}{x^A} \frac{I(x_s^B, \theta_s)}{x_s^B} \sigma_{\gamma\gamma} (1 - \cos \theta_s) dx^A dx_s^B d\Omega. \end{aligned} \quad (14)$$

where the bulk-frame charge densities are denoted by a prime. The rate pair creation induced by side-scattering of soft photons per unit volume,

$$\frac{\partial}{\partial t} (\Gamma n'_{e^+}) + \nabla \cdot (\Gamma \beta c n'_{e^+}) = \int N_{\text{mult}} \frac{F_x(x^A)}{x^A} \frac{I(x_s^B, \theta_s)}{x_s^B} \sigma_{\gamma\gamma} (1 - \cos \theta_s) dx^A dx_s^B d\Omega. \quad (15)$$

The Compton force acting on transrelativistic or subrelativistic particles has been neglected.

Substituting the equations of continuity into (14) yields

$$\frac{d\Gamma\beta}{dt} = \frac{\partial\Gamma\beta}{\partial t} + c\boldsymbol{\beta} \cdot \nabla(\Gamma\beta) = \frac{1}{m_e(2\mu_e n_{e^+} + m_p n_p) c^5} \int \left[(x^A + x^B) f - \left(\frac{\mu_e}{m_e} \right) N_{\text{mult}} 2\Gamma\beta \right] \frac{F_x(x^A)}{x^A} \frac{I(x_s^B, \theta_s)}{x_s^B} \sigma_{\gamma\gamma} (1 - \cos \theta_s) dx^A dx_s^B d\Omega. \quad (16)$$

The value of the second term in the brackets depends on the importance of secondary pair creation. During the last stages of acceleration ($f \simeq \frac{5}{3}$) one has $\mu_e \simeq m_e$ and $N_{\text{mult}} \simeq 1$ (§2.2). Otherwise, we substitute $f = 1$ and expression (13) for N_{mult} , and find that the quantity in brackets is $(x^A + x^B)$ multiplied by $(1 - \frac{1}{3})/(1 + \beta)$. Both these results can be expressed in terms of a β -dependent Compton afterburn parameter

$$f_\beta = \begin{cases} \frac{5}{3} & \text{(no secondary pair creation);} \\ \frac{1-\beta/3}{1+\beta} & \text{(secondary pair creation).} \end{cases} \quad (17)$$

The photon shell will be parameterized by a radial coordinate ϖ , measured from its inner boundary,

$$r = c(t - \Delta t) + \varpi. \quad (18)$$

The scattering occurs at position ϖ_s and time t_s , and the collision at position ϖ_\pm and time t_\pm . Hence,

$$\varpi_s - \varpi_\pm = c(t_\pm - t_s) \cos \theta_s. \quad (19)$$

The intensity $I(x_s^B, \theta_s)$ of side-scattered photons is related to the flux $F_x(x^B)$ of unscattered radiation in the thin shell (cf. eq. [2]) via

$$I(x_s^B, \theta_s, \varpi_\pm) = \int_{\varpi_\pm}^{c\Delta t} (2n_{e^+} + n_p) F_x(x^B) (1 - \beta) \frac{d\sigma}{d\Omega} \exp \left[-\tau_{\gamma\gamma}(x_s^B, \theta_s, \varpi_s - \varpi_\pm) \right] d\varpi_s. \quad (20)$$

Note that the radial position ϖ_s of the scattering site within the photon shell always lies outside the position ϖ_\pm of pair creation, because the radial speed of the side-scattered photon is less than c . The optical depth to pair creation experienced by the side-scattered photon is

$$\tau_{\gamma\gamma}(x_s^B, \theta_s, \varpi_s - \varpi_\pm) = \int_{\varpi_s}^{\varpi_\pm} \frac{d\varpi'}{c} \int_{x_{\min}^A(x_s^B, \theta_s)}^{\infty} dx^A \frac{F_x(x^A)}{x^A} (1 - \cos \theta_s) \sigma_{\gamma\gamma} \left[x^A / x_{\min}^A(x_s^B, \theta_s) \right]. \quad (21)$$

When the optical depth along the ray from ϖ_\pm to ϖ_s is much larger than unity, the momentum deposited by side-scattering and pair creation is localized, and the x^A -integral can be performed directly:

$$\frac{d}{dt}(\Gamma\beta) = \frac{f_\beta}{\mu c^2} \int ((x^A) + x^B) F_x(x^B) (1 - \beta) d\sigma \frac{dx_s^B}{x_s^B}, \quad (22)$$

where we have made use of eq. (5) for the mean mass μ per scattering charge. The average energy of the undeflected, radial photon is

$$\langle x^A \rangle \equiv \frac{\int F_x(x^A) \sigma_{\gamma\gamma} dx^A}{\int F_x(x^A) \sigma_{\gamma\gamma} dx^A / x^A}, \quad (23)$$

after weighting by cross-section and photon-spectrum. We write

$$\langle x^A \rangle(x_s^B, \theta_s) = k(\alpha) x_{\min}^A(x_s^B, \theta), \quad (24)$$

from here on. The constant k is plotted as a function of high energy spectra index in Fig. 1.

It is now necessary to prescribe the radiation spectrum. We assume a simple broken power-law form, appropriate for GRB sources, with photon number flux (per logarithm of energy) constant below a break energy $x_{\text{br}} \sim 1$ and photon index α above the break:

$$F_x(x^A) = \begin{cases} F_x(x_{\text{br}}) & x^A < x_{\text{br}}; \\ F_x(x_{\text{br}}) \left(x^A/x_{\text{br}}\right)^{-\alpha+1} & x^A > x_{\text{br}}. \end{cases} \quad (25)$$

For the assumed spectral shape, low energy photons ($x < x_{\text{br}}$) are side-scattered at a slightly higher rate than are photons near the break energy x_{br} (the scattering cross-section is not KN-suppressed). These low energy photons then pair produce off photons of energy $x \gg x_{\text{br}}$, and deposit a relatively large momentum. It will be convenient to introduce the modified parameter

$$\tau'_c = \tau_c \times \frac{x_{\text{br}} F_{x_{\text{br}}}}{F} = \sigma_T \Delta t \frac{x_{\text{br}} F_{x_{\text{br}}}}{m_e c^2}, \quad (26)$$

which rescales τ_c by the ratio of the energy flux at frequency x_{br} to the total energy flux.

The energy of the side-scattered photon cannot, however, be taken to be arbitrarily small. When $x_s^B \ll 1$, the radiation shell becomes optically thin to pair creation. This leads to an *upper* bound on the energy of the photo-pair, which we now evaluate. Each side-scattered photon overlaps the shell for a time $\sim \Delta t / (1 - \cos \theta_s)$, but the collision rate is proportional to $(1 - \cos \theta_s) \sigma_{\gamma\gamma}$. The optical depth to pair creation therefore depends on θ_s only implicitly through x_{\min}^A :

$$\begin{aligned} \tau_{\gamma\gamma}(x_s^B, \theta_s) &= \frac{\Delta t}{m_e c^2} \int_{x_{\min}^A(x_s^B, \theta_s)}^{\infty} dx^A \frac{F_x(x^A)}{x^A} \sigma_{\gamma\gamma} \left[x^A / x_{\min}^A(x_s^B, \theta_s) \right] \\ &\equiv k_2(\alpha) F_x \left[x_{\min}^A(x_s^B, \theta_s) \right] \frac{\sigma_T \Delta t}{m_e c^2} > 1. \end{aligned} \quad (27)$$

The dimensionless function k_2 is plotted against spectral index α in Fig. 1. Defining a characteristic optical depth τ'_c (eq. [26]) through the photon shell at frequency x_{br} , and noting that in general $x_{\min}^A \gg x_{\text{br}}$, one gets an upper bound on the mean energy $x^{\text{pair}} = \langle x^A + x^B \rangle \simeq \langle x^A \rangle$,

$$\frac{x_{\max}^{\text{pair}}}{x_{\text{br}}} = k \left[k_2 \frac{\tau'_c}{x_{\text{br}}} \right]^{1/(\alpha-1)}. \quad (28)$$

This upper bound is approximately independent of the scattering θ_s (even though the most probable energy of the side-scattered photon that collides to form a pair of energy x_{\max}^{pair} does depend on θ_s). The corresponding lower bound on the energy of the scattered photon is

$$x_s^B > \frac{2k}{x_{\max}^{\text{pair}}(1 - \cos \theta_s)} \sim \frac{4k\Gamma^2}{x_{\max}^{\text{pair}}}. \quad (29)$$

This energy sits below (above) the break energy x_{br} when Γ is less than (greater than) $2\Gamma^*$, where

$$\Gamma^* = \frac{1}{4k^{1/2}} (x_{\text{br}} x_{\max}^{\text{pair}})^{1/2}. \quad (30)$$

Thus, the supply of side-scattered photons is smaller when $\Gamma > 2\Gamma^*$, and the acceleration rate is reduced accordingly.

We first calculate the acceleration at low Lorentz factors, $\Gamma \ll \Gamma^*$. The softness of the side-scattered photons allows us to perform the integral (22) over x_s^B in the Thomson regime, $dx_s^B/x_s^B = dx^B/x^B$. At this stage of the acceleration, $\langle x^A \rangle = x_{\max}^{\text{pair}} \gg x^B$. Setting a lower bound (29) to x_s^B , we obtain

$$\frac{d}{dt}(\Gamma\beta) \simeq \frac{f_\beta x_{\max}^{\text{pair}} F_x(x_{\text{br}})}{m_e c^2} \left(\frac{m_e}{\mu} \right) (1 - \beta) \int d\sigma, \quad (31)$$

and we have

$$\frac{d}{dt}(\Gamma\beta) = f_\beta \tau'_c \left(\frac{x_{\max}^{\text{pair}}}{x_{\text{br}}} \right) \left(\frac{m_e}{\mu} \right) \frac{1 - \beta}{\Delta t} \quad (\Gamma \ll \Gamma^*). \quad (32)$$

It is worth recalling the physical origin of the various factors in this expression: f_β is the Compton afterburn parameter (eq. [17]) which describes the influence of secondary Compton scattering and pair creation on the net momentum injected per high energy pair; τ'_c (eq. [26]) is a dimensionless parameter, proportional to the energy flux at frequency x_{br} and comparable to the optical depth to $\gamma - \gamma$ collisions through the photon shell; x_{\max}^{pair} (eq. [28]) is the maximum energy of the injected pair in the lab frame (above which the optical depth to pair creation through the shell is small); μ (eq. [5]) is the mean inertia per scattering charge; and Δt is the temporal width of the photon shell.

To approach the high-Lorentz factor regime (where $\Gamma \gg 2\Gamma^*$) we approximate the scattering charges as being cold, $\langle \gamma_e \rangle = 1$ and $\mu_e = m_e$. This approximation turns out to be justified, as in this regime the time for freshly injected pairs to Compton cool in the bulk frame is short compared with the acceleration time (§2.2). Since the minimum value of x^B lies above x_{br} , the frequency dependence of F_x gives an additional factor of

$$\frac{1}{\alpha} \left[\frac{x_{\max}^{\text{pair}} x_{\text{br}} (1 - \beta)(1 - \cos \theta_s)}{2k(1 - \beta \cos \theta_s)} \right]^{\alpha-1} \quad (33)$$

after performing the integral over x_s^B . Here, the factor in brackets is x_{br} divided by the minimum value of x^B before scattering (eqs. [6] and [29]). After substituting the relation $(1 - \cos \theta_s)/(1 -$

$\beta \cos \theta_s) = (1 - \cos \theta'_s)/(1 + \beta)$, the acceleration rate can be expressed as

$$\frac{d}{dt}(\Gamma\beta) = \frac{2f_\beta k}{\alpha} \left(\frac{x_{\text{br}} x_{\text{max}}^{\text{pair}}}{2x_{\text{br}} k} \right)^\alpha \frac{F_x(x_{\text{br}})}{m_e c^2} (1 - \beta) \int d\Omega' \left[(1 - \cos \theta'_s) \frac{1 - \beta}{1 + \beta} \right]^{\alpha-1} \frac{d\sigma}{d\Omega'}, \quad (34)$$

which becomes

$$\frac{d}{dt}(\Gamma\beta) = f_\beta \tau'_c \left(\frac{x_{\text{max}}^{\text{pair}}}{x_{\text{br}}} \right) \left(\frac{\Gamma^*}{\Gamma} \right)^4 \frac{1}{2(\Gamma^*)^2 \Delta t} \quad (\Gamma \gg \Gamma^*) \quad (35)$$

for $\alpha = 2$. This expression matches onto (32) at $\Gamma = \Gamma^*$.

Let us compare the rates of acceleration just derived with the corresponding expression

$$\frac{d\Gamma}{dr} = \Gamma^2 (1 - \beta)^2 \tilde{\ell} \frac{R}{r^2}. \quad (36)$$

for Thomson scattering without pair creation (Noerdlinger 1974; Paper I). When $1 \ll \Gamma \ll \Gamma^*$, the acceleration rate (32) is larger by $\sim 2f_\beta x_{\text{max}}^{\text{pair}}$ than for Thomson scattering by a spectrum localized near x_{br} ; and when $\Gamma \gg \Gamma^*$ the acceleration rate (35) is larger by $\sim 2f_\beta x_{\text{max}}^{\text{pair}} (\Gamma/\Gamma^*)^{-2}$.

Pair creation no longer increases the speed of the bulk flow when two colliding photons of comparable energy, $x^B \sim x^A \sim 2k/x_s^B (1 - \cos \theta_s) \sim x_{\text{max}}^{\text{pair}}$ have an optical depth to pair creation that is close to unity. The resulting maximum Lorentz factor is

$$\Gamma_{\text{max}}^{\text{pair}} \sim \frac{x_{\text{max}}^{\text{pair}}}{\sqrt{2k}} = \left(\frac{k}{2} \right)^{1/2} \left[k_2 x_{\text{br}}^{\alpha-2} \tau'_c \right]^{1/(\alpha-1)}. \quad (37)$$

Continued scattering in the pair-loaded flow increases its speed further: the limiting Lorentz factor is

$$\Gamma_{\text{max}} \simeq \frac{1}{2} \tau_c, \quad (38)$$

from eq. (1). This is comparable to (37) for $\alpha = 2$, but larger for softer high energy spectra. We conclude that the main effects of pair creation are i) to increase the rate of acceleration at low Lorentz factor; and ii) to reduce the mean mass per scattering charge to $\mu \simeq m_e$, thereby allowing much higher terminal Lorentz factors.

2.2. Mean Energy of the Pairs in the Bulk Frame

It remains to calculate the mean energy $\langle \gamma_e \rangle$ of the pairs in the bulk frame, and show that our starting assumption that $\langle \gamma_e \rangle \ll x_{\text{max}}^{\text{pair}}$ is self-consistent. During the first stages of acceleration an electron or positron will be injected with a characteristic energy $\gamma_e^{\text{max}} \sim \frac{1}{2} x_{\text{max}}^{\text{pair}}$, and will cool off the radial photon flux when $x_{\text{br}} \ll x_{\text{max}}^{\text{pair}}$. At the same time, the accelerated medium is compressed (Paper I), and the pairs are adiabatically heated at a rate $\langle \gamma_e \rangle^{-1} (d\langle \gamma_e \rangle / dt) = \frac{1}{3} n'^{-1} (dn' / dt) = \frac{1}{3} \Gamma^{-1} (d\Gamma / dt)$. The equilibrium energy $\langle \gamma_e \rangle$ that results from a balance between compressional heating and Compton cooling lies far below the injection energy, and so we will assume that the

heating process has isotropized the momenta of the pairs in the bulk frame. From eq. (38) of Paper I,

$$\langle \gamma_e \rangle = \frac{1}{2} \left(\frac{t_{\text{cool}}^0}{t_{\text{accel}}^0} \right)^{1/2}, \quad (39)$$

where the reference (lab-frame) cooling time is $t_{\text{cool}}^0 = m_e c^2 / \sigma_T \Gamma F_\Gamma \simeq (\Gamma / 2\tau_c') \Delta t$, and $F_\Gamma \simeq F / 2\Gamma^2$ is the energy flux in the boosted frame. The acceleration rate is decreased by a factor $\sim \langle \gamma_e \rangle^{-1}$ from the values (32) and (35) calculated above for a cold plasma:

$$\frac{1}{\Gamma} \frac{d\Gamma}{dt} \simeq \frac{1}{\langle \gamma_e \rangle t_{\text{accel}}^0}. \quad (40)$$

For a spectrum $\alpha = 2$,

$$\frac{t_{\text{cool}}^0}{t_{\text{accel}}^0} = \frac{f_\beta x_{\text{max}}^{\text{pair}}}{4\Gamma^2} = \frac{4f_\beta k}{x_{\text{br}}^2} \left(\frac{\Gamma}{\Gamma^*} \right)^{-2} \quad (41)$$

at $1 \ll \Gamma \ll \Gamma^*$, and

$$\frac{t_{\text{cool}}^0}{t_{\text{accel}}^0} = \frac{4f_\beta k}{x_{\text{br}}^2} \left(\frac{\Gamma}{\Gamma^*} \right)^{-4} \quad (42)$$

at $\Gamma \gg \Gamma^*$. The equilibrium Lorentz factor works out to $\langle \gamma_e \rangle \simeq 1.4\Gamma^{-1} (x_{\text{max}}^{\text{pair}}/100)^{1/2}$ for a pair-loaded plasma moving slowly ($\Gamma < \Gamma^*$).

2.3. Relative Inertia in Pairs and Baryons

The distribution of inertia between (cold) pairs and baryons within the accelerated material has important implications for the radiative efficiency of the forward shock. The number of pairs multiplies greatly as each hard e^\pm (of bulk frame energy $\gamma_e \sim x_{\text{max}}^{\text{pair}}/4\Gamma$) cools by side-scattering the photon beam. During the initial stages of the acceleration, the side-scattered photons are well above the pair creation threshold; little additional momentum is absorbed from the photon beam when they collide with soft photons. The momentum imparted to the medium by the cooling of the hard e^\pm is cancelled. In this regime, $f \simeq 1$.

Balancing the radial momentum density in the lab frame, under the assumption that each injected hard pair leads to $N_{\text{mult}} \gg 1$ softer pairs with an isotropic distribution in the bulk frame, we obtain

$$x_{\text{max}}^{\text{pair}} \frac{n_{e^+}}{N_{\text{mult}}} m_e c = \Gamma (2\mu_e n_{e^+} + m_p n_p) c. \quad (43)$$

Here, $\mu_e = \frac{4}{3} \langle \gamma_e \rangle m_e$ when the pairs are at least mildly relativistic and the multiplicity N_{mult} is given by $x_{\text{max}}^{\text{pair}}/4\Gamma \langle \gamma_e \rangle$ (eq. [13]). This equation inverts to

$$\frac{2n_{e^+} \mu_e}{m_p n_p} = 2. \quad (44)$$

The medium becomes very heavily loaded by pairs as it accelerates to bulk relativistic speed (where $\langle \gamma_e \rangle \simeq 1$). The fraction of the inertia carried by the hadrons becomes

$$f_h = \frac{m_p n_p}{2\mu_e n_{e^+} + m_p n_p} \simeq \frac{1}{3} \quad (45)$$

in this regime.

Compton scattering of photons of lab-frame energy $\sim x_{\text{br}}$ by the hard e^\pm is initially in the Klein-Nishina regime, where the e^\pm loses a significant fraction of its energy in one scattering. Cooling continues in the KN regime as long as $\gamma_e^2(x_{\text{br}}/2\Gamma) > \gamma_e$, that is, as long as $\Gamma < (2k)^{1/2}\Gamma^*$. As the medium attains a Lorentz factor not far below the maximum value (38), the hard e^\pm are injected with a small enough bulk frame energy that most of the energy lost to Compton cooling is *not* reabsorbed by photon collisions. This occurs when $\gamma_e^2(x_{\text{br}}/2\Gamma)(x_{\text{max}}^{\text{pair}}/2\Gamma) < 1$, that is, when $(\Gamma/\Gamma_{\text{max}})^4 > \frac{1}{4} k^3 k_2^{3/(\alpha-1)} (\tau'_c/x_{\text{br}})^{(7-4\alpha)/(\alpha-1)}$. Above this Lorentz factor, $f \simeq \frac{5}{3}$.

Implicit in this calculation of the maximum Lorentz factor is the assumption that the photon flux is high enough to supply the needed momentum. This constraint translates into an upper bound on the density of the medium surrounding the γ -ray source. The strongest constraint comes from the requirement that the phase of pair-dominated acceleration continues up to a Lorentz factor $\Gamma_{\text{max}}^{\text{pair}}$ (eq. [37]). This sets a lower bound to the flux of photons of energy $\sim x_{\text{max}}^{\text{pair}}$.

3. Shock Deceleration, Pulse Broadening, and Afterglow

We now turn to consider the effects of radiative acceleration on the dynamics of a decelerating, relativistic fireball. The emission process operating in a GRB probably covers a range of radius. In some models, the emission is due to optically thin synchrotron and/or inverse-Compton processes (Mészáros, Rees, & Papathanassiou 1994; Sari, Piran, & Narayan 1998); whereas in others the emission is by inverse-Compton scattering at moderate Compton optical depth (Thompson 1994, 1997; Crider et al. 1997). To focus the present discussion, we assume that the dissipation extends outward from (at least moderately) large optical depth. The optical depth τ_c (eq. [3]) through the photon shell is

$$\tau_c = \tau_c^0 \left(\frac{R}{R_\tau} \right)^{-2}, \quad (46)$$

outside the scattering photosphere. Here, R_τ is the radius at which the ejecta become optically thin to scattering and the γ -ray photons begin to stream ahead of the matter. As long as pair creation and annihilation remain in equilibrium at energy $x \sim 1$ in the bulk frame ($x \sim \Gamma_{\text{ej}}$ in the lab frame), the position of the Thomson photosphere is determined implicitly by⁴

$$F_x(\Gamma_{\text{ej}} x_{\text{br}}) \frac{\sigma_T \Delta t}{m_e c^2} = \frac{\tau'_c}{x_{\text{br}}} \left(\frac{\Gamma_{\text{ej}}}{x_{\text{br}}} \right)^{-\alpha} \sim 1. \quad (47)$$

⁴Here α is the high-energy spectral index; eq. (25).

(Recall that τ'_c is τ_c rescaled by the factor $x_{\text{br}}F_{x_{\text{br}}}/F$.) In this way, the initial value of τ_c can be related to the (initial) bulk Lorentz factor of the ejecta,

$$\tau'_c{}^0 \sim (\Gamma_{\text{ej}}^0)^{\alpha-1} x_{\text{br}}^{2-\alpha}. \quad (48)$$

This equation provides an upper bound on $\tau'_c{}^0$ if the γ -ray emission region is optically thin to scattering.

The width of the prompt γ -ray pulse is bounded below by

$$\Delta t \geq \frac{R_\tau}{2c(\Gamma_{\text{ej}}^0)^2}. \quad (49)$$

More generally, we can define a minimum timescale for variability driven by internal dissipation in the outflow,

$$\Delta t_{\text{var}}(R) = \frac{R}{2c\Gamma_{\text{ej}}^2}. \quad (50)$$

This timescale can be related to the γ -ray fluence $\partial E/\partial\Omega$ (at energy x_{br} and per unit solid angle) by noting that

$$\tau'_c{}^0 = \sigma_T \frac{\partial E/\partial\Omega}{m_e c^2 R_\tau^2}. \quad (51)$$

At the scattering photosphere, one finds

$$\Delta t_{\text{var}}(R_\tau) = 0.5 \left(\frac{x_{\text{br}}}{300}\right)^{(\alpha-2)/2} \left[\frac{4\pi(\partial E/\partial\Omega)}{10^{53} \text{ erg}}\right]^{1/2} \left(\frac{\Gamma_{\text{ej}}^0}{300}\right)^{-(3+\alpha)/2} \text{ s} \quad (52)$$

upon making use of eq. (48). Should the overall duration Δt of the burst be determined by the activity of the central engine, one does not expect the afterglow emission to connect up smoothly with the main burst. However, the internal dissipation could be triggered by an interaction with the external medium: for example, when a blob of magnetized ejecta is decelerated and the causal propagation distance within the blob grows large enough to allow reconnection (Thompson 1994; Begelman 1998). In such a hybrid model, the observation of distinct, overlapping sub-pulses requires that the ejecta extend over a cone of angular width $\theta \gg (\Gamma_{\text{ej}}^0)^{-1}$, and that the surface of the ejecta is wrinkled on angular scales larger than $\sim (\Gamma_{\text{ej}}^0)^{-1}$. To simplify the discussion that follows, we assume that the burst is composed of a single pulse of width $\Delta t \sim R_\tau/2(\Gamma_{\text{ej}}^0)^2 c$.

3.1. Deceleration of the Ejecta

Pre-acceleration of the ambient medium by the prompt γ -ray pulse will slow the deceleration of the burst ejecta, and therefore modify the synchrotron emission from the forward shock. The maximum Lorentz factor (eq. [38]) to which the ambient medium may be accelerated decreases

with distance from the matter photosphere. Let us assume, for the time being, that the ambient material is light enough to allow acceleration to $\Gamma_{\text{amb}} = \Gamma_{\text{max}}$. Then

$$\Gamma_{\text{amb}}(R) = \Gamma_{\text{max}}(R_\tau) \left(\frac{R}{R_\tau} \right)^{-2}, \quad (53)$$

since $\Gamma_{\text{max}} \propto \tau_c \propto R^{-2}$. Thus, the kinetic energy per scattering charge behind the forward shock is

$$\frac{\Gamma_{\text{ej}}^2(R)}{\Gamma_{\text{amb}}(R)} \mu c^2, \quad (54)$$

in the lab frame. Here, $\mu = m_e/(1 - f_h)$ (eq. [5]) is the mean mass per scattering charge.

The energy E of the shock decreases with radius, because only a fraction f_h of the post-shock particle energy is carried by baryons that do not cool. The calculation in §2.3 indicates that the inertia of the ambient medium becomes dominated by leptons (eq. 45). Energy is deposited in shocked leptons at a rate

$$\frac{\partial^2 E_\pm}{\partial \Omega \partial t} = -(1 - f_h) \frac{\Gamma_{\text{ej}}^2}{\Gamma_{\text{amb}}} \frac{m_p}{f_h} n_{p0}(R) R^2 c^3. \quad (55)$$

We assume that these particles cool instantly. When $f_h \ll 1$, the remaining energy E of the fireball is dominated by the kinetic energy of the ejected matter (mass M_0),

$$\frac{\partial E}{\partial \Omega} = \Gamma_{\text{ej}} \frac{\partial M_0}{\partial \Omega} c^2. \quad (56)$$

One can calculate the time-scaling of the shock energy by balancing the energy radiated (55) against the energy retained (56). Assuming the density profile around the center of the explosion to be a powerlaw

$$n_{p0}(R) = \frac{\rho_0(R)}{m_p} \propto R^{-\delta}, \quad (57)$$

one finds

$$E(R) \propto R^{-\epsilon}, \quad (58)$$

with

$$\epsilon = 5 - \delta. \quad (59)$$

This compares with $\epsilon \simeq 3 - \delta$ in the case where the external medium is static or moves subrelativistically (e.g. Katz & Piran 1997).

More generally we will assume a power-law scaling (58) of the shock energy. This assumption is motivated by the weak dependence of f_h (eq. [45]) on the gamma-ray continuum in the region where acceleration to bulk relativistic speed is possible. At large radius $f_h \rightarrow 1$ and $\epsilon \rightarrow 0$, because pairs with the minimum (shock-frame) energy $\sim \Gamma_{\text{ej}} m_e c^2$ no longer cool effectively. This allows a first evaluation of the influence of radiative acceleration and pair loading on the initial stages of

the deceleration of a relativistic shock. A more detailed numerical treatment of shock deceleration including these effects is deferred to a later paper.

Balancing the shock energy with the energy deposited in shocked particles, one obtains

$$\Gamma_{\text{ej}}(R) = \Gamma_{\text{ej}}(R_\tau) \left(\frac{R}{R_\tau} \right)^{(\delta-\epsilon-5)/2}. \quad (60)$$

The relation between shock radius and observed (post-burst) time t becomes

$$t \propto R^{6-\delta+\epsilon}. \quad (61)$$

Pair creation feeds back strongly on the radiative losses from a relativistic outflow, and regions with extended non-thermal spectra are expected to be much brighter than regions with quasi-thermal (e.g. Wien) spectra (Thompson 1997). It also introduces new characteristic lengthscales and time-scales into the afterglow process. One of these is the radius $R(\Gamma_{\text{amb}} \sim 1)$ outside of which the ambient medium is accelerated to sub-relativistic speeds. If the medium were to remain pair loaded out to this radius, one would calculate $R(\Gamma_{\text{amb}} \sim 1)$ by setting $\mu \sim m_e$ in eq. (1); this would yield $R(\Gamma_{\text{amb}} \sim 1)/R_\tau \sim (\frac{1}{2}\tau_c)^{1/2}$. However, because several efoldings of the pair density are required to push the ambient medium (assumed initially free of pairs) to bulk relativistic speed, bulk relativistic motion effectively stops somewhat inside that radius. A more accurate estimate of $R(\Gamma_{\text{amb}} \sim 1)$ is obtained by noting that when τ_c is not much larger than unity, the pair density exponentiates according to $n_{e^+}/n_p \sim \exp(n_\gamma \sigma_T c \Delta t) = \exp(\tau_c/x_{\text{br}})$. Requiring that $2m_e n_{e^+} \sim m_p n_p$ yields $\tau_c/x_{\text{br}} \sim \ln(m_p/2m_e) \sim 7$. This value of τ_c is large enough that the photon shell is optically thick to photon collisions, $\tau_{\gamma\gamma} \sim 0.25\tau_c/x_{\text{br}} \sim 2$. Pairs continue to dominate baryons in number out to a radius where $\tau_c/x_{\text{br}} \sim 1$; but are not produced in sufficient numbers to force the mean inertia per scattering charge down to $\mu \sim m_e$. The corresponding delay from the beginning of the burst is given by the time it takes the forward shock to reach that radius. In the case of a uniform external medium, $\Gamma_{\text{ej}} \propto R^{-5/2}$ and the time delay scales with radius as $R/2\Gamma_{\text{ej},c}^2 \propto R^6$. This yields

$$\frac{\Delta t(\Gamma_{\text{amb}} \sim 1)}{\Delta t} \sim \left(\frac{\tau_c^0}{10} \right)^3 \sim 3 \times 10^4 \left(\frac{\tau_c^0}{300} \right)^3. \quad (62)$$

3.2. Synchrotron Emission

This pre-acceleration of the ambient medium will modify the time-scaling of the synchrotron emission from the forward shock propagating ahead of the burst ejecta. The pair-loading ensures that the Lorentz factor of the shock-accelerated particles (in the shock frame) extends downward to the minimum kinematically allowed value, $\gamma_e \sim \Gamma_{\text{ej}}$ (Thompson 1997). We consider here only the simplest emission model involving synchrotron radiation by a power-law distribution of pairs,

$\partial n_e / \partial \gamma_e \propto \gamma_e^{-P}$ for rest frame energies

$$\gamma_e > \frac{\Gamma_{\text{ej}}}{\Gamma_{\text{amb}}}. \quad (63)$$

Closely related synchrotron models, in which the inertia of the non-thermal particles is dominated by baryons, have been constructed by Mészáros & Rees (1997), Wijers, Rees & Mészáros (1997) and Waxman (1997). The energy carried by the non-thermal pairs is taken to be a constant fraction ε_{cr} of the total post-shock particle energy in the shock frame, and the magnetic field is assumed to carry a constant fraction ε_B of the post-shock pressure. As we discuss below, pre-acceleration of the ambient medium by a collimated γ -ray beam will ensure that this second assumption is satisfied, once the ejecta are moving sufficiently slowly.

The medium just ahead of the shock is compressed at the same time as it is accelerated, so that the lab-frame density of baryonic particles has increased to $n_p \simeq 2\Gamma_{\text{amb}}^2 n_{p0}$ over the ambient value (eq. [17] of paper I). The bulk frame energy density behind the shock is, then

$$\left(\frac{\Gamma_{\text{ej}}}{\Gamma_{\text{amb}}} \right)^2 2n_{e+} \mu c^2 \simeq \frac{2\Gamma_{\text{ej}}^2}{f_h} n_{p0} m_p c^2. \quad (64)$$

The equilibrium post-shock magnetic pressure therefore scales as

$$\frac{B_r^2}{8\pi} \propto \varepsilon_B \Gamma_{\text{ej}}^2 n_{p0} \propto R^{-5-\epsilon}, \quad (65)$$

independent of δ in the shock rest frame.

We are now in a position to work out the time-scaling of the synchrotron emission at fixed frequency ν . Pairs which radiate at this frequency (Lorentz-boosted into the observer's frame) have an energy

$$\gamma_e \sim \left(\frac{2\pi\nu m_e c}{\Gamma_{\text{ej}} e B_r} \right)^{1/2} \propto R^{5/2 - (\delta - 2\epsilon)/4}. \quad (66)$$

When synchrotron cooling is rapid, the synchrotron emissivity depends on the incoming flux of kinetic energy, but not explicitly on post-shock magnetic field. Assuming an powerlaw spectrum $\partial N_e / \partial \gamma_e \propto \gamma_e^{-P}$ of injected particles, the energy released in photons of frequency ν is, per unit time

$$\frac{\nu}{R^2} \frac{\partial L_\nu}{\partial \Omega} \simeq \Gamma_{\text{ej}}^2 \left[\varepsilon_{\text{cr}} \left(\frac{\gamma_e}{\Gamma_{\text{ej}} / \Gamma_{\text{amb}}} \right)^{2-P} 2\Gamma_{\text{ej}}^2 n_{p0}(R) \frac{m_p c^3}{f_h} \right]. \quad (67)$$

The quantity in brackets denotes the rate at which particle energy accumulates (in the bulk frame) per unit area of the shock; the prefactor transforms to the lab frame. The power law index

$$\beta \equiv - \frac{\partial \ln(\nu L_\nu)}{\partial \ln t} \quad (68)$$

is expressed in terms of the synchrotron index $\alpha_{\text{sync}} = \frac{1}{2}P$ via

$$\beta = \frac{6\alpha_{\text{sync}} + 2 - \frac{1}{2}\delta(3\alpha_{\text{sync}} - 1) + 2\epsilon\alpha_{\text{sync}}}{6 - \delta + \epsilon} \quad (\Gamma_{\text{amb}} = \Gamma_{\text{max}}; \text{ fast cooling}). \quad (69)$$

When the shock loses energy slowly ($\epsilon \simeq 0$), one has $\beta = \alpha_{\text{sync}} + \frac{1}{3}$ for a uniform medium ($\delta = 0$) and $\beta = \frac{3}{4}\alpha_{\text{sync}} + \frac{3}{4}$ for a steady wind ($\delta = 2$).

Now let us compare this result for the time-scaling of the synchrotron emission, with the corresponding expression for a shock propagating into a *static* external medium. In that more familiar case, the shock Lorentz factor, observer's time, and rest-frame magnetic field scale as $\Gamma_{\text{ej}} \propto R^{(\delta-\epsilon-3)/2}$, $t \propto R^{1/(4-\delta+\epsilon)}$, $B_r \propto R^{-3/2-\epsilon/2}$, and $\gamma_e \propto R^{3/2-(\delta-2\epsilon)/4}$. For those scalings, the time index is

$$\beta = \frac{6\alpha_{\text{sync}} - 2 - \frac{1}{2}\delta(3\alpha_{\text{sync}} - 1) + 2\epsilon\alpha_{\text{sync}}}{4 - \delta + \epsilon} \quad (\Gamma_{\text{amb}} = 1; \text{ fast cooling}). \quad (70)$$

This agrees with the scaling previously obtained whose energy decreases by Sari et al. (1998) and Mészáros et al. (1998) if we substitute expression (59) for ϵ (in the case of a strongly radiative shock); or $\epsilon = 0$ (in the case of an almost adiabatic shock). An adiabatic shock has $\beta = \frac{3}{2}\alpha_{\text{sync}} - \frac{1}{2}$ for any value of δ .

The regime of slow synchrotron cooling (at the observed frequency ν) is treated analogously. We can now assume $\epsilon = 0$, because the lowest energy e^\pm must not be able to cool in this regime. One has

$$\nu \frac{\partial L_\nu}{\partial \Omega} \propto \left(\gamma_e \frac{\partial^2 N_e}{\partial \gamma_e \partial \Omega} \right) \Gamma_{\text{ej}}^2 \gamma_e^2 B_r^2, \quad (71)$$

where the total number of radiating charges is

$$\gamma_e \frac{\partial^2 N_e}{\partial \gamma_e \partial \Omega} \simeq \frac{1}{3 - \delta} R^3 n_{p0}(R) \epsilon_{cr} \frac{m_p}{f_h m_e} \left(\frac{\gamma_e}{\Gamma_{\text{ej}}/\Gamma_{\text{amb}}} \right)^{1-P}. \quad (72)$$

The relation between synchrotron index and particle index softens to $\alpha_{\text{sync}} = (P - 1)/2$, and the time index becomes identical to (69):

$$\beta = \frac{6\alpha_{\text{sync}} + 2 - \frac{1}{2}\delta(3\alpha_{\text{sync}} - 1)}{6 - \delta} \quad (\Gamma_{\text{amb}} = \Gamma_{\text{max}}; \text{ slow cooling}) \quad (73)$$

for $\epsilon = 0$. Notice that the functional dependence of the time-index β on the spectral index α_{sync} remains the same for both fast and slow synchrotron cooling, when the ambient medium has been pre-accelerated by the prompt γ -ray pulse and the lowest energy e^\pm do not cool radiatively ($\epsilon \simeq 0$). If the injected spectrum of non-thermal particles is constant – let us take $P = 2$ – then across a ‘cooling break’ the spectrum hardens from $\alpha_{\text{sync}} = 1$ to $\alpha_{\text{sync}} = \frac{1}{2}$ and the time index hardens from $\beta = (8 - \delta)/(6 - \delta)$ to $(5 - \frac{1}{4}\delta)/(6 - \delta)$.

By contrast, there is a stronger break in the time scaling between regimes of fast and slow cooling if the external medium is static,

$$\beta = \frac{6\alpha_{\text{sync}} - \frac{1}{2}\delta(3\alpha_{\text{sync}} - 1)}{4 - \delta} \quad (\Gamma_{\text{amb}} = 1; \text{ slow cooling}). \quad (74)$$

(Mészáros et al. 1998). This simplifies to the familiar result $\beta = \frac{3}{2}\alpha_{\text{sync}}$ in a uniform external medium. For $P = 2$, the time index hardens from $\beta = 1$ to $\beta = (3 - \frac{1}{4}\delta)/(4 - \delta)$ across the ‘cooling break’.

3.3. Anisotropic Radiation Pressure and Shearing of External Magnetic Fields

The prompt γ -ray pulse induces strong shearing motions in the ambient medium that can amplify a seed magnetic field before the forward shock hits. An important question, that has yet to be resolved in afterglow models, regards the effectiveness with which a weak ambient magnetic field (e.g. $B_{\text{ex}} \sim 3\mu$ G for a fireball interacting with the ISM) will be amplified above the flux density $\sim \Gamma_{\text{ej}}^2 B_{\text{ex}}$ expected from laminar compression behind a relativistic shock. In the non-relativistic limit (where pair creation can be neglected), the limiting speed of the ambient medium is proportional to the γ -ray flux. One therefore expects the flow outside the forward shock to be strongly sheared on lengthscales in between $(\Gamma_{\text{ej}}^0)^{-1}R$ and $\theta_{\text{beam}}R$, given that the γ -ray emission is beamed within an angle θ_{beam} but also varies on the smaller angular scale due to causal fluctuations in the rate of internal dissipation. This sheared flow will be Kelvin-Helmholtz unstable and, if there is time before the shock hits, the resulting turbulence will strongly tangle a seed magnetic field. Since the available time is $\sim R/2\Gamma_{\text{ej}}^2 c$, one expects effective tangling only after the ejecta have decelerated below $\Gamma_{\text{ej}} \sim (\Gamma_{\text{ej}}^0)^{1/2}$. Thereafter, near equipartition between the magnetic pressure and the turbulent pressure in the sheared flow appears plausible: $B \sim (4\pi n_{p0} m_p c^2)^{1/2} \sim 0.1 (n_{p0}/1 \text{ cm}^{-3})^{1/2}$ G. If no other instability (such as a two-stream instability; Medvedev & Loeb 1999) raises the field close to equipartition, one expects the burst and/or afterglow lightcurves to contain features correlated with the onset of effective magnetic shearing.

3.4. Upper Bound on Pre-Burst Mass Loss: Pulse Broadening

A strong constraint on the density of the ambient medium comes from the requirement that the accelerated matter (which becomes loaded with pairs) remain optically thin to Compton scattering, so that the γ -ray pulse is not appreciably broadened. This becomes a serious constraint even if the scattering optical depth through the ambient medium is small (cf. §3.3 of Paper I). If all photons of frequency $> x$ are converted to pairs, then the scattering depth through the resulting shell of pairs is

$$\tau_T \simeq \frac{\tau'_c}{x_{\text{br}}} \left(\frac{x}{x_{\text{br}}} \right)^{1-\alpha} = \frac{\tau_c'^0}{x_{\text{br}}} \left(\frac{R}{R_\tau} \right)^{-2} \left(\frac{x}{x_{\text{br}}} \right)^{1-\alpha}. \quad (75)$$

In order to prevent photons of this energy from being completely consumed, the medium must be accelerated sufficiently that the photons are no longer above the threshold energy for pair-creation in the bulk frame.⁵ To maintain $\tau_T < 1$, we require that

$$\Gamma_{\text{amb}} > \Gamma_\tau(R) \equiv \left[\tau_c'(R) x_{\text{br}}^{\alpha-2} \right]^{1/(\alpha-1)}. \quad (76)$$

⁵The material undergoing radiative acceleration remains in causal contact with itself, and so the scattering depth through it is not affected by the suppression of the scattering rate (by a factor $\sim 1 - \beta$) in the lab frame.

The critical Lorentz factor Γ_τ can be expressed more directly in terms of the initial bulk Lorentz factor of the ejecta, after making use of eq. (48):

$$\frac{\Gamma_\tau(R)}{\Gamma_{\text{ej}}^0} \simeq \left(\frac{R}{R_\tau}\right)^{-2/(\alpha-1)}. \quad (77)$$

Note that Γ_τ coincides with Γ_{ej}^0 at the scattering photosphere. If $\Gamma_{\text{amb}} < \Gamma_\tau$, then the γ -ray pulse is spread out to a width

$$\frac{\Delta t_{\text{spread}}}{\Delta t} = \frac{R}{2\Gamma_{\text{amb}}^2 c \Delta t} \simeq \left(\frac{\Gamma_{\text{amb}}}{\Gamma_\tau}\right)^{-2} \left(\frac{R}{R_\tau}\right)^{(\alpha+3)/(\alpha-1)}. \quad (78)$$

One finds that $\Delta t_{\text{spread}} > \Delta t$ at $R \geq R_\tau$.

The kinetic energy of the accelerated medium moving at Lorentz factor Γ_τ (within a shell of thickness equal to the acceleration length $\frac{2}{3}\Gamma_\tau^2 c \Delta t$; eq. [2]) can be no larger than the energy of the γ -ray pulse above a frequency $x \sim \Gamma_\tau$,

$$\Gamma_\tau n_p n_0 m_p c^2 \left(1 + 2 \frac{n_{e^+} m_e}{n_p m_p}\right) \frac{2}{3} \Gamma_\tau^2 c \Delta t \leq \left(\frac{F_{x_{\text{br}}} x_{\text{br}}}{c}\right) \left(\frac{\Gamma_\tau}{x_{\text{br}}}\right)^{1-\alpha} c \Delta t. \quad (79)$$

This yields the upper bound

$$\rho_0 < \frac{3x_{\text{br}}^{(5-2\alpha)/(\alpha-1)}}{2(\tau_c')^{3/(\alpha-1)}} \left(\frac{m_e}{\sigma_T c \Delta t}\right) \left(1 + 2 \frac{n_{e^+} m_e}{n_p m_p}\right)^{-1} \propto \left(\frac{R}{R_\tau}\right)^{6/(\alpha-1)}. \quad (80)$$

The density in the above equation is higher than that encountered in the diffuse ISM, and therefore does not provide any constraint on GRB models involving the merging of compact objects. We can use this expression, however, to set limits on massive stars as likely GRB progenitors, as in this case the explosion occurs in a dense pre-burst stellar wind. Assuming a steady mass loss from such a massive progenitor at a rate \dot{M} and constant speed V , the ambient density is

$$\rho_0(R) = \frac{\dot{M}}{4\pi R^2 V}. \quad (81)$$

Substituting this expression into eq. (80), and making use of eqs. (48) and (49) to express R_τ in terms of Δt , $\tau_c'^0$ and x_{br} , we have

$$\dot{M} < 24\pi f_h \left(x_{\text{br}}^{2\alpha-3} \tau_c'^0\right)^{1/(\alpha-1)} \frac{m_e c V \Delta t}{\sigma_T} \left(\frac{R}{R_\tau}\right)^{(2\alpha+4)/(\alpha-1)}. \quad (82)$$

Setting $\Gamma_{\text{amb}} = \Gamma_\tau$ and eliminating R , one deduces that the amount of pre-burst mass loss needed to induce a certain spreading of the pulse is

$$\frac{\dot{M}}{\dot{M}_{\Delta t}} = \left(\frac{\Delta t_{\text{spread}}}{\Delta t}\right)^{(2\alpha+4)/(3+\alpha)}. \quad (83)$$

where

$$\begin{aligned} \dot{M}_{\Delta t} &\equiv 24\pi f_h x_{\text{br}} \Gamma_{\text{ej}}^0 \left(\frac{m_e c V \Delta t}{\sigma_T} \right) \\ &= 1.5 \times 10^{-5} x_{\text{br}} f_h \left(\frac{\Gamma_{\text{ej}}^0}{300} \right) \left(\frac{\Delta t}{10 \text{ s}} \right) \left(\frac{V}{1000 \text{ km s}^{-1}} \right) M_{\odot} \text{ yr}^{-1}. \end{aligned} \quad (84)$$

Notice that both the width Δt_{spread} of the spread pulse (eq. [49]) and $\dot{M}_{\Delta t}$ grow with radius R . Mass loss rates close to the critical value $\dot{M}_{\Delta t}$ only broaden the γ -ray pulse near the scattering photosphere, and do not broaden it by much. Higher mass loss rates cause further broadening at larger radii.

The presence of a dense medium surrounding the GRB source also limits the bulk Lorentz factor Γ_{ej}^0 of the ejecta at the Thomson photosphere. Hence the width Δt of the emitted γ -ray pulse (before scattering in the ambient medium) cannot be made arbitrarily small. An upper bound to Γ_{ej}^0 is obtained by balancing the energy of the ejecta with the kinetic energy of the baryons accumulating behind the shock:

$$\frac{1}{\varepsilon_{\text{rad}}} \frac{\partial E}{\partial \Omega} \geq \frac{(\Gamma_{\text{ej}}^0)^2}{3 - \delta} \rho_0 (R_{\tau}) R_{\tau}^3 c^2. \quad (85)$$

Here ε_{rad} is the fraction of the kinetic energy of the ejecta converted to γ -rays; this expression is meant to be evaluated at the scattering photosphere of the outflow, and so is missing the factor of Γ_{amb}^{-1} present in eq. [56]. Combining this equation with (48) and (51), one finds

$$\Gamma_{\text{ej}}^0 \leq \left(\frac{4\pi V}{\varepsilon_{\text{rad}} \dot{M} c^2} \right)^{2/(5-\alpha)} \left(\frac{\partial E}{\partial \Omega} \frac{m_e c^2}{\sigma_T} x_{\text{br}}^{2-\alpha} \right)^{1/(5-\alpha)}, \quad (86)$$

or

$$\Gamma_{\text{ej}}^0 \leq 36 \varepsilon_{\text{rad}}^{-2/3} \left(\frac{\dot{M}}{10^{-5} M_{\odot} \text{ yr}^{-1}} \right)^{-2/3} \left(\frac{V}{1000 \text{ km s}^{-1}} \right)^{2/3} \left[\frac{4\pi(\partial E/\partial \Omega)}{10^{53} \text{ erg}} \right]^{1/3} \quad (87)$$

for a hard spectrum $\alpha = 2$. The width of the broadened pulse becomes

$$\Delta t \geq \frac{R_{\tau}}{2(\Gamma_{\text{ej}}^0)^2 c} \geq \frac{1}{2c} \left(\frac{\varepsilon_{\text{rad}} \dot{M} c^2}{4\pi V} \right)^{(3+\alpha)/(5-\alpha)} \left(\frac{\partial E}{\partial \Omega} \right)^{(1-\alpha)/(5-\alpha)} \left(\frac{m_e c^2}{\sigma_T} x_{\text{br}}^{2-\alpha} \right)^{-4/(5-\alpha)}. \quad (88)$$

Evaluating this expression for $\alpha = 2$, we deduce

$$\Delta t \geq 170 \varepsilon_{\text{rad}}^{5/3} \left(\frac{\dot{M}}{10^{-5} M_{\odot} \text{ yr}^{-1}} \right)^{5/3} \left(\frac{V}{1000 \text{ km s}^{-1}} \right)^{-5/3} \left[\frac{4\pi(\partial E/\partial \Omega)}{10^{53} \text{ erg}} \right]^{-1/3} \text{ s}. \quad (89)$$

We can combine this last result with eq. (83) to obtain a very similar bound on the width of the scattered γ -ray pulse:

$$\frac{\Delta t_{\text{spread}}}{\Delta t} = \left(\frac{1}{3f_h x_{\text{br}} \varepsilon_{\text{rad}}} \right)^{(\alpha+3)/(2\alpha+4)} \Gamma_{\text{ej}}^{(\alpha+3)(\alpha-2)/(2\alpha+4)(5-\alpha)}. \quad (90)$$

Note that the width of the scattered pulse is independent of Γ_{ej} for a hard spectrum $\alpha = 2$, $\Delta t_{\text{spread}}/\Delta t = 2.2 (f_h x_{\text{br}} \varepsilon_{\text{rad}}/0.1)^{-5/8}$. It is much larger than Δt for softer spectra, e.g., $\Delta t_{\text{spread}}/\Delta t = 2.1 \Gamma_{\text{ej}}^{3/10} (f_h x_{\text{br}} \varepsilon_{\text{rad}}/0.1)^{-3/5}$ for $\alpha = 3$. Because the softer spectrum creates fewer pairs, a larger external mass density is required to induce runaway pair creation for a fixed shock energy.

This calculation sets significant constraints on GRB models involving the delayed explosions of massive Wolf-Rayet stars (Woosley 1993; MacFadyen & Woosley 1998), whose winds are characterized by mass loss rates $\dot{M} \approx 10^{-5} - 10^{-4} M_{\odot} \text{ yr}^{-1}$ and velocities of 1000–2500 km s⁻¹ (Willis 1991). Hard bursts composed of peaks narrower than ~ 10 sec must either form in a more rarefied environment, or have a low radiative efficiency ε_{rad} . The possibility remains that the overall duration of some γ -ray bursts is determined by the processes of pair-loading and radiative acceleration in the ambient medium. We note finally that the constraint (89), (90) is weakened if the γ -ray source function is not a rigid power-law, but has a thermal cutoff below a bulk frame energy $\sim m_e c^2$.

4. Discussion

We have calculated the deposition of radiative momentum into an (initially) static medium by the intense γ -ray pulse emanating from a relativistic fireball (eqs. [32] and [35]). This process loads the accelerated medium with pairs, which come to dominate its inertia (eq. 44); and greatly increases the radiative efficiency of the forward shock wave that bounds the fireball material. Given this high radiative efficiency, the ambient medium will attain a bulk Lorentz factor close to the Lorentz factor of the fireball material near the γ -ray photosphere, decreasing as R^{-2} at larger radius (eq. [53]). As a result, the rate of deceleration of the ejecta is slowed (eq. [60]), and the relation between the time-index of the synchrotron emission and the synchrotron spectral index (eqs. [69] and [73]) is modified from the relation previously obtained for a static ambient medium.

These physical processes have important implications for the radiative physics of the forward shock, aside from its overall radiative efficiency. Anisotropy in the γ -ray flux (on an angular scale Γ^{-1} or larger) will induce shearing motions in the external medium that can strongly amplify any seed magnetic field before the shock hits it (§3.3). An even more important effect is that the minimum Lorentz factor of the shocked pairs is pushed down to $\gamma_e \sim 1$ in the bulk frame, so that the corresponding synchrotron break frequency lies at optical-UV near the e^{\pm} scattering photosphere. This may point to a hybrid radiative mechanism (Thompson 1997) in which hard X-ray photons advected out with the fireball are the principal seeds for Comptonization by non-thermal pairs and bulk fluid motions.

Support for this work was provided by the Sloan foundation (C. T.), and by the NSF through grant PHY94-07194 (P. M.). We thank A.M. Beloborodov for discussions, and the referee for suggesting a number of improvements to the presentation.

REFERENCES

- Baring, M.G. & Harding, A.K. 1997, *ApJ*, 491, 663
- Beloborodov, A.M. 1999, *MNRAS*, 305, 181
- Crider, A., Liang, E. P., Smith, I. A., Preece, R. D., Briggs, M. S., Pendleton, G. N., Paciesas, W. S., Band, D. L., & Matteson, J. L. 1997, *ApJ*, 497, L39
- Jauch, J. M. & Rohrlich, F. 1976, *The Theory of Photons and Electrons* (New York: Springer-Verlag)
- Katz, J. & Piran T. 1997, *ApJ*, 490, 772
- MacFadyen, A. & Woosley, S. E. 1998, preprint (astro-ph/9810274)
- Madau, P. & Thompson, C. 1999, *Ap J*, in press (paper I)
- Medvedev, M.V., & Loeb, A. 1999, preprint (astro-ph/9904363)
- Mészáros, P., Rees, M. J., & Papathanassiou, H. 1994, *ApJ*, 432, 181
- Mészáros, P., & Rees, M. J. 1997, *ApJ*, 476, 232
- Mészáros, P. Rees, M. J., & Wijers, R. A. M. J. 1998, *ApJ*, 499, 301
- Noerdlinger, P. D. 1974, *ApJ*, 192, 529
- O’Dell, S. L. 1981, *ApJ*, 243, L147
- Phinney, E. S. 1982, *MNRAS*, 198, 1109
- Sari, R., Piran, T., & Narayan, R. 1998, *ApJ*, 497, L17
- Thompson, C. 1994, *MNRAS*, 270, 480
- Thompson, C. 1997, in *Relativistic Jets in AGN*, ed. M. Ostrowski, M. Sikora, G. Madejski, & M. Begelman, Krakow, p. 63
- Waxman, E. 1997, *ApJ*, 485, L5
- Wijers, R. A. M. J., Rees, M.J., & Mészáros, P. 1997, *MNRAS*, 288, L51
- Willis, A. J. 1991, in *Wolf-Rayet Stars and Interrelations with Other Massive Stars in Galaxies*, ed. K. A. van der Hucht & B. Hidayat (Dordrecht: Kluwer), 256
- Woosley, S. E. 1993, *ApJ*, 405, 273

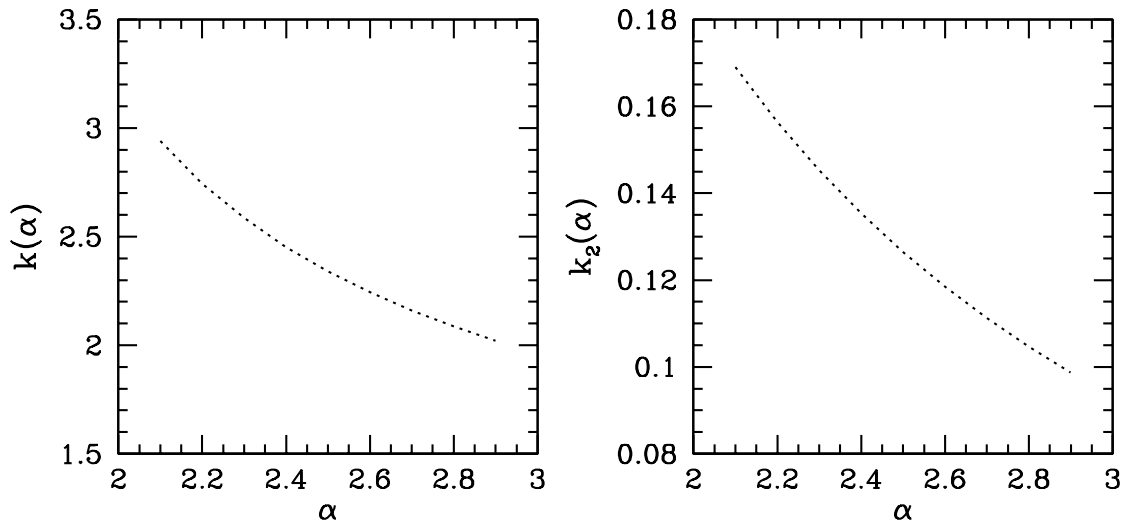


Fig. 1.— *Left:* The function $k(\alpha)$ (eq. [24]), plotted against spectral index α . *Right:* The function $k_2(\alpha)$ (eq. [27]).